Electromagnetic Bandgap (EBG) Structure Using Open Stubs to Suppress Power Plane Noise

Hiroshi Toyao[*1], Noriaki Ando[*2]

[*] *System Jisso Research Laboratories, NEC Corporation*
1120, Shimokuzawa, Sagamihara, Kanagawa 229-1198, Japan

[1]h-toyao@bc.jp.nec.com

[2]n-ando@bu.jp.nec.com

***Abstract*— We have developed a novel electromagnetic bandgap (EBG) structure for suppressing power plane noise that enables unit cell size to be miniaturized by using open stubs as shunt circuits. Since stub length determines the center frequencies of stopbands for this structure, reduced implementation area can be anticipated while maintaining stopbands at lower frequencies. Stopband frequencies were estimated by dispersion analysis based on the Bloch theorem. Highly suppressed noise propagation over the estimated frequencies was validated by full-wave simulation and demonstrated experimentally.**

Key words: Electromagnetic bandgap (EBG) structures, power planes, noise suppression, printed circuit boards.

I. INTRODUCTION

Power plane noise excited by simultaneous switching of digital processors or memories is becoming a significant problem for high-speed digital systems. Particularly in wireless communication equipments combining digital and RF systems, power plane noise propagating between power and ground planes causes serious throughput reduction. From the viewpoint of efficient frequency band usage for wireless communication, power plane noise must be effectively isolated from the RF section. Recently, new ideas have been proposed for suppressing power plane noise by using electromagnetic bandgap (EBG) structures in printed circuit boards (PCBs) [1]-[3].

Fig. 1 shows a cross-sectional view of a conventional EBG structure. In this structure, the conductive top and bottom plane pair forms a natural parallel-plate waveguide (PPW). In the inner layer, conductive square patches are arrayed periodically with lattice constant *a*. The center of each conductive patch is connected to the bottom plane through a conductive via. The structure separated by the dashed lines shown in Fig. 1 represents a unit cell of the periodical structure.

The power plane noise excited by digital circuits is considered to propagate through the PPW as a TEM-mode wave. Fig. 2 shows a simplified equivalent circuit model based on [4] for a unit cell assuming TEM-mode wave propagation. In the figure, L_{PPW} and C_{PPW} are respectively the PPW inductance and capacitance for one unit cell and L_{via} and C_{patch} are respectively the inductance of the via that connects the patch to the bottom plane and the capacitance between the top plane and the patch.

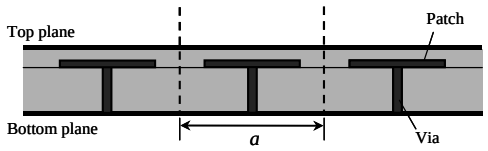

Fig. 1. Cross- sectional view of conventional EBG structure

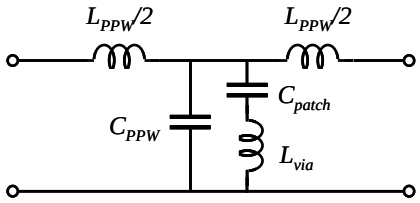

Fig. 2. Equivalent circuit of a unit cell for a conventional EBG structure

As shown in Fig. 2, a unit cell of a conventional EBG structure can be modeled as a PPW shunted by an LC series resonance circuit. The stopband center frequencies are given by the series resonant frequencies where the shunt circuit behaves as a short circuit. To shift the stopbands to a lower frequency, it is necessary to increase L_{via} or C_{patch} by increasing via length or patch size. Consequently, enlarged unit cell size is inevitable in a conventional EBG structure. Therefore, it is highly desired to develop a structure that is compact and able to maintain a stopband at a lower frequency to apply EBG structures to densely implemented PCBs.

In this paper, we propose a new EBG structure that makes it possible to miniaturize unit cell size by using open stubs rather than patches as shunt circuits.

II. EBG STRUCTURE USING OPEN STUBS

A. Structure Design and Equivalent Circuit

Fig. 3 shows the top view (a) and cross-sectional view (b) of our proposed EBG structure. As can be seen in Fig. 3(b), the conductive top and bottom plane pair forms a PPW parallel to the *xy*-plane. In the surface layer above the top plane, open stubs are arrayed in the two-dimensional periodic lattice with lattice constant *a* as shown in Fig. 3(a). Each open stub consists of a transmission line of length *d* and width *w* using the top plane as the current return path. One end of each open stub is connected to the bottom plane by a conductive

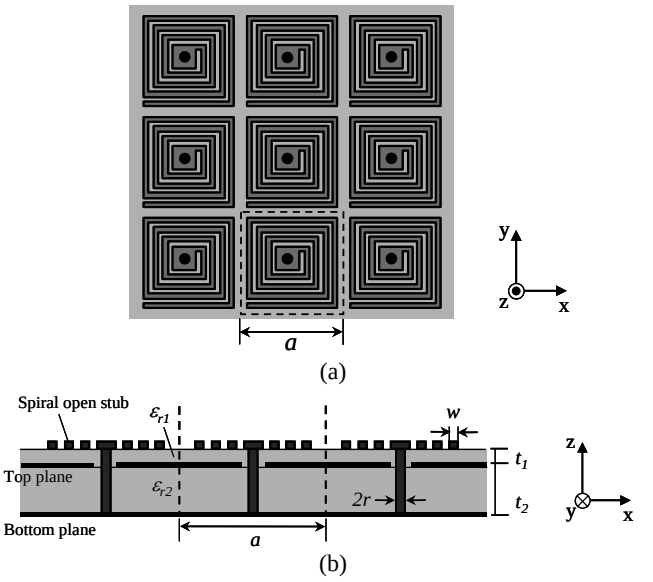

Fig. 3. Top view (a) and cross-sectional view (b) of proposed EBG structure.

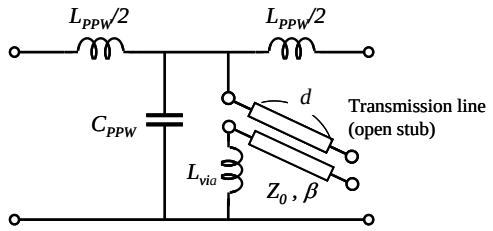

Fig. 4. Equivalent circuit of the unit cell for proposed EBG structure

via through the clearance of the top plane. The area surrounded by the dashed lines in the figure corresponds to the unit cell of our proposed structure. The upper dielectric layer located on the top plane has thickness t_1 and relative dielectric constant ε_{r1}. In addition, the lower dielectric layer located between the top and bottom planes has thickness t_2 and relative dielectric constant ε_{r2}. Due to the miniaturization of the implementation area, the open stubs appear as spiral shapes in Fig. 3, but shapes such as straight and meandering ones can also be used.

Fig. 4 shows an equivalent circuit model of the unit cell for our proposed structure assuming TEM-mode wave propagation in the *x*-direction. In this circuit, L_{PPW} and C_{PPW} respectively represent the PPW inductance and capacitance for one unit cell and L_{via} is the inductance of the via that connects the open stub to the bottom plane. The transmission line of length *d*, characteristic impedance Z_0, and phase constant β corresponds to the open stub. As the figure shows, the unit cell of our proposed EBG structure can be modeled as a PPW shunted by a series circuit comprising an open stub and L_{via}.

B. Estimates of Stopband Frequencies

The center frequencies of the stopbands for our EBG structure are given by the resonant frequencies where the admittance *Y* of the shunt circuit is $\pm\infty$.

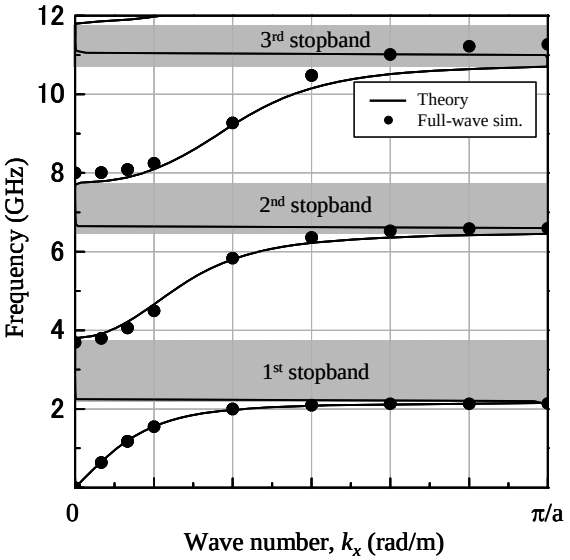

Fig. 5. Dispersion diagram for proposed EBG structure in Fig. 3 with a = 2.5mm, t_1 = 0.06mm, t_2 = 0.4mm, w = 0.1mm, d = 18.2mm, r = 0.15mm, ε_{r1} = ε_{r2} = 4.2.

The admittance *Y* is calculated as

$$Y = \frac{i\tan(\beta d)}{Z_0 - \omega L_{via}\tan(\beta d)} \tag{1}$$

where ω is radian frequency. The phase constant β of the transmission line in (1) is given by

$$\beta = \frac{\omega}{c}\sqrt{\varepsilon_{eff}} \tag{2}$$

where c is the speed of light in a vacuum and ε_{eff} is the effective relative dielectric constant of the transmission line. According to (1), the admittance *Y* is described as a function of the transmission line length *d*, so that the center frequencies of the stopbands can be designed by changing the stub length *d*. In addition, the center frequencies can be made lower merely by making the stub length longer, with small implementation area. This is the major advantage of our proposed EBG structure with respect to miniaturizing unit cell size in comparison with the conventional EBG structure.

Furthermore, not only for estimating center frequencies but also the upper and lower limit frequencies of stopbands, we can calculate the dispersion relation of the EBG structure. As the following formula shows, the dispersion relation can be obtained by using a periodic boundary condition based on the Bloch theorem for the equivalent unit cell circuit depicted in Fig. 4.

$$\cos(k_x a) = \omega L_{PPW}\left(\frac{\tan(\beta d)}{\omega L_{via}\tan(\beta d) - Z_0} - \omega C_{PPW}\right)\Big/2 + 1 \tag{3}$$

In this equation, k_x is the wave number of the TEM-mode wave that propagates in the *x*-direction of the EBG structure. Fig. 5 shows a dispersion diagram that represents the relation

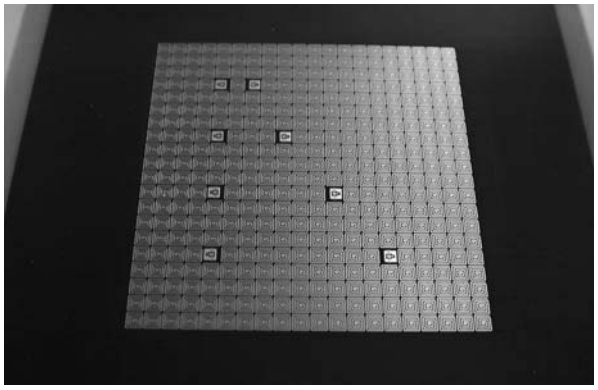

Fig. 6. Sample board with proposed EBG structure. Four pairs of ports are located within the EBG structure. The pair ports are separated by 1, 3, 6, and 9 cells respectively.

between frequency $f = \omega / 2\pi$ and wave number k_x for our proposed EBG structure with a = 2.5mm, t_1 = 0.06mm, t_2 = 0.4mm, w = 0.1mm, d = 18.2mm, r = 0.15mm, and $\varepsilon_{r1} = \varepsilon_{r2}$ = 4.2.

In Fig. 5, the solid lines represent the results calculated from (3) and the dots represent the full wave simulation (HFSS) results obtained using the periodic boundary condition for unit cell model analysis. We obtained excellent agreement between the calculated and simulated results up to 10 GHz. The right edge of Fig. 5 corresponds to the edge of the first Brillouin zone, where the wave meets the Bragg condition. As shown in the figure, the lowest dispersion curve (defined as the first passband) starts from the coordinate origin with a positive slope. The first stopband appears at a frequency of 2.15 GHz, where the first passband reaches the first Brillouin zone edge. The second passband starts at 3.81 GHz, which is the upper limit frequency of the first stopband. The second stopband appears between 6.43 GHz and 7.75 GHz. Above this frequency, passbands and stopbands appear alternately as frequency increases. This characteristic can be explained by periodic impedance conversion of the admittance Y shown in (1).

III. Board Design and Experiments

Sample boards were fabricated to validate the effectiveness of our EBG structure and to compare the stopband characteristics of calculated and experimental data. Fig. 6 shows an overall view of a sample board. Its parallel-plate dimensions are 100 mm × 100 mm. 20 × 20 unit cells were arranged in the center of the parallel plate with a = 2.5 mm, t_1 = 0.06 mm, t_2 = 0.4 mm, w = 0.1 mm, d = 18.2 mm, and r = 0.15mm, which are the same parameters as in Fig. 5. The commonly-used FR4 substrate having a relative dielectric constant ε_r = 4.2 was used for the upper and lower dielectric layers. As shown in Fig. 6, there are four pairs of ports in the board and the two ports in each pair are separated by 1, 3, 6, and 9 cells respectively. Each port is comprised of signal and ground probing pads on the surface layer that are connected to the top and bottom plane by conductive vias respectively. The insertion loss (S_{21}) between the two ports was measured with a vector network analyzer (VNA).

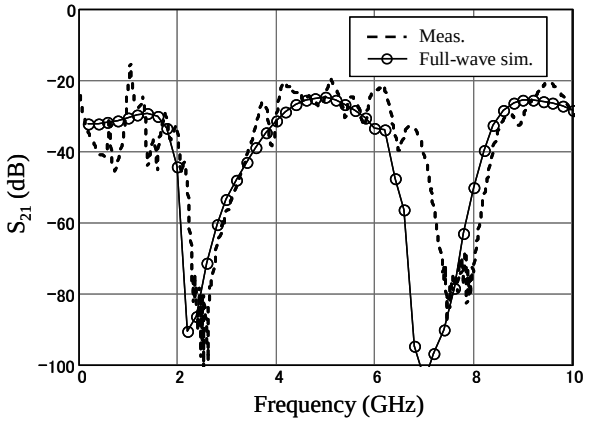

Fig. 7. Measured and full-wave simulation insertion loss (S_{21}) between ports separated by six cells for the EBG structure shown in Fig. 3 with the same parameters as in Fig. 5.

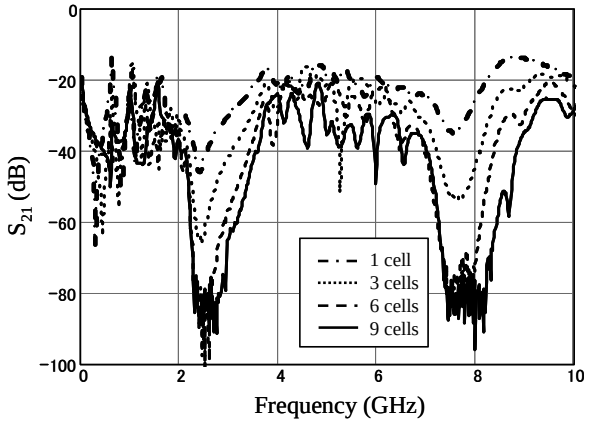

Fig. 8 Dependence of measured insertion loss (S_{21}) on the number of cells between ports for the EBG structure shown in Fig. 3 with the same parameters as in Fig. 5.

Fig. 7 shows the measured and simulated results of the insertion loss between the pair of ports separated by six cells. From the figure, it can be seen that the first and second stopbands occur at around 2.5 GHz and 7.6 GHz respectively. We obtained good agreement between measured and simulated results over the frequency range up to 5 GHz, which includes the first stopband. The measured frequency values for the first stopband were also found to agree well with the calculated values (2.15 GHz to 3.81 GHz) shown in Fig. 5. These results show that the stopband frequency can be estimated accurately by using dispersion analysis. In contrast, the measured frequency values for the second stopband were several hundred MHz higher than the simulated and calculated results (6.43 GHz to 7.75 GHz). This disparity can be explained as being due to the differences between the actual dimensions and the design dimensions used for the dispersion analysis and full-wave simulation. The reason for this is that

the effect of dimension error becomes especially significant at higher frequencies.

Fig. 8 shows the dependence of the measured insertion loss on the number of unit cells between the ports. The stopband edges become steeper and the insertion loss increases as the number of cells increases. It is particularly significant that for the case when the ports are separated by nine cells, the measured insertion loss was well below the noise floor which was around –80 dB. This leads us to conclude that in this case the wave propagation was almost completely suppressed.

IV. Conclusion

We have developed a novel EBG structure using open stubs as the shunt admittance for suppressing power plane noise. The stopband frequencies are estimated by dispersion analysis based on the Bloch theorem for unit cells. High suppression of noise propagation over the estimated frequency range was validated by full-wave simulation and demonstrated experimentally. With our structure it is possible to reduce stopband frequencies merely by increasing the stub lengths. This gives it a substantial advantage over the conventional EBG structure with respect to miniaturizing unit cell size.

Acknowledgment

This work has been supported by the Ministry of Internal Affairs and Communications.

References

[1] R. Abhari and G. V. Eleftheriades, "Metallo-dielectric electromagnetic bandgap structures for suppression and isolation of the parallel-plate noise in high –speed circuit," *IEEE Trans. Microw. Theory Tech.*, vol. 51, no. 6, pp. 1629-1639, Jun. 2003.

[2] S. Shahparnia, O. M. Ramahi, "Electromagnetic interference (EMI) reduction from printed circuit boards (PCBs) using electromagnetic bandgap structures," *IEEE Trans. Electromagn. Compat.*, vol. 46, no. 4, pp. 580-587, Nov. 2004.

[3] Tzong-Lin Wu, Yen-Hui Lin, Sin-Ting Chen, "A novel power planes with low radiation and broadband suppression of ground bounce noise using photonic bandgap structures," *IEEE Microw. Wireless Compon. Lett.*, vol. 14, no. 7, pp. 621-623, July 2004.

[4] S. D. Rogers, "Electromagnetic-bandgap layers for broad-band suppression of TEM modes in power planes," *IEEE Trans. Microw. Theory Tech.*, vol. 53, no. 8, pp. 2495-2505, Aug. 2005.